Characterization of solid polymer electrolyte based on gum tragacanth and lithium nitrate

Jenova I, Venkatesh K, Karthikeyan S, Madeswaran S, Arivanandhan M & Joice Sheeba D

Published online: 23 Jun 2021.

Submit your article to this journal ⎘

View related articles ⎘

View Crossmark data ⎘

Taylor & Francis
Taylor & Francis Group

Check for updates

Characterization of solid polymer electrolyte based on gum tragacanth and lithium nitrate

Jenova I[a,b], Venkatesh K[a,b], Karthikeyan S [a], Madeswaran S[c], Arivanandhan M[d], and Joice Sheeba D[a]

[a]Department of Physics, Madras Christian College, Chennai, Tamil Nadu, India; [b]University of Madras, Chennai, Tamil Nadu, India; [c]Centre for Functional Materials(CFM), Vellore Institute of Technology (VIT), Vellore, Tamil Nadu, India; [d]Centre for Nanoscience and Technology, Anna University, Chennai, Tamil Nadu, India

ABSTRACT

Tragacanth Gum is a natural gum that has been widely used in food, pharmaceutical, and cosmetic industries. The electrochemical properties of the gum have not been explored yet. Therefore, in the present work solid polymer electrolytes based on Gum Tragacanth (GT) and Lithium nitrate (LN) have been synthesized by solution casting method. The dissociation and complexation of the salt with the host polymer are confirmed using XRD and FTIR studies. Impedance analysis was carried out using electrochemical impedance spectroscopy (EIS) in the temperature range of 308–343 K. The highest ionic conductivity at room temperature is found to be 8.28×10^{-3} Scm^{-1}. The temperature dependence of the system GT:LN was found to obey Arrhenius behavior. Dielectric studies were carried out using impedance spectroscopy in the frequency range 10 Hz-4 MHz. Transference number study showed that the main charge carriers were ions and electrochemical stability window for the highest conducting electrolyte was studied using Linear sweep voltammetry. Thermogravimetry studies showed that thes electrolytes are thermally stable.
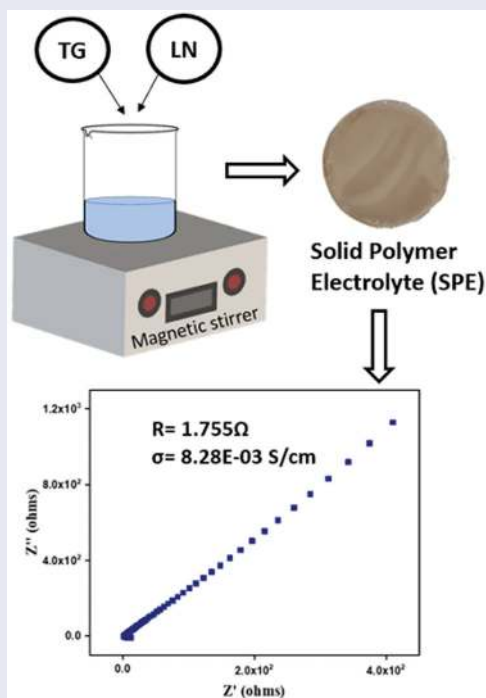
1. Introduction

Research toward solid state devices has grown to a larger extent in the past years due to the increasing demand toward smart energy storage devices. Solid polymer electrolytes (SPE) that play a vital role in electrochemical devices have an upper hand when compared to the liquid electrolytes, due to its flexibility, electrochemical

CONTACT Karthikeyan Shunmugavel ✉ karthisrivi@gmail.com ▣ Department of Physics, Madras Christian College, East Tambaram 600059, Chennai, Tamil Nadu, India

stability, safety and its ability to form proper electrode–electrolyte interface.[1] The use of biopolymers in solid polymer electrolytes has gained enormous significance with the hope of producing biodegradable and bio compactible films to tackle the environmental crisis. Their abundance in nature, low cost, and nontoxic nature are added factors that make them more suitable to be used as SPE. Several biopolymer electrolytes such as cellulose acetate,[2] agar,[3] chitosan,[4] carrageenan[5] have been reported with good ionic conductivity that is suitable for electrochemical devices.

In this work, we use a new natural Gum-based polymer, Tragacanth (GT) whose electrochemical studies have not been explored yet. Gum Tragacanth is one of the most widely used natural gum obtained from the stems and branches of Asiatic species of *Astragalus*.[6] Tragacanth is a highly branched, heterogenous, and anionic carbohydrate that consists of two major components, a water swellable part – bassorin and a water-soluble part – Tragacanthin that forms a colloidal hydrosol. Tragacanthin is composed of tragacantic acid (ethanol-insoluble) which contains residues of D-galacturonic acid, D-xylose, L-fucose, and D-galactose and arabinogalactan (ethanol-soluble minor fraction) containing residues of L-arabinose, D-galactose, and D-galacturonic acid.[6–9] Tragacanth gum is used in pharmaceutical industry, food products, cosmetics, antimicrobial, and biomedical applications.[10]

There have been no reports on its electrochemical application and hence in our present work we aim to produce a solid biopolymer electrolyte based on tragacanth gum as a host polymer.

Lithium salts are considered as good proton donors and SPE prepared using biopolymers and lithium salts have shown good ionic conductivity.[11–15] Lithium nitrate is selected as the lithium source for doping in gum tragacanth. In the present work, the structural, vibrational, mechanical and electrical properties of gum tragacanth doped with different concentration of LiNO$_3$ have been presented.

2. Materials and methods

In our current study, films of Tragacanth gum-based polymer electrolytes were prepared using solution casting technique. Gum tragacanth (GT) and lithium nitrate (LN) salt were mixed in proper weight ratio as presented in Table 1. The solvent used here is distilled water. The solution mixtures were stirred continuously using a magnetic stirrer for 24 hours to get a clear homogenous solution. The solutions were then poured into polypropylene petri dishes and were left to dry at 50°C until solid films were formed. A homogenous free-standing film is shown in Figure 1.

X-ray diffraction studies were carried out using Bruker D8 Advanced X-ray diffractometer with Cu Kα radiation. FTIR measurements were performed using SHMADZU IR Affinity-1. The ionic conductivity study of the polymer electrolytes has been carried out in the temperature range of 308–343 K over a frequency range of 10 Hz to 4 MHz using HIOKI 3536 LCR meter. Transference number was measured using Wagner's polarization method. The electrochemical stability of the electrolyte was analyzed by linear sweep voltammetry using Biologic potentiostat VSP 300. The thermal stability of the samples was analyzed using thermogravimetric analysis using SDT Q600 V20.9 Build 20.

3. Results and discussion

3.1. XRD analysis

Figure 2(P) shows the X-ray diffraction pattern of pure GT. Previous reports have shown that the XRD pattern of pure gum tragacanth exhibits a broad hump in the range 2θ = 19⁰ and a sharp microcrystalline peak in the range 2θ = 28⁰ indicating the microcrystalline structure of GT, due to intra-hydrogen bonding.[10,16,17] In our present study, the microcrystalline peak is absent whereas the characteristic broad diffraction hump is observed at 2θ = 20⁰ which indicates the amorphous nature of the host polymer matrix. Figure 2(A-D) shows the diffraction pattern of the different salt complexes of GT. As seen from the figure, the amorphous peak broadens with increasing salt concentration, thus proving that the addition of LiNO$_3$ decreases the degree of crystallization.

The relative degree of crystallinity (χ_c) can be calculated from the following equation:

$$\chi_c = \frac{A_c}{A_t} \times 100\% \tag{1}$$

where A_c is the area under the crystalline peak and A_t is the total area under both the crystalline and amorphous peaks.

The χ_c values are tabulated in Table 2. The χ_c value obtained from the pure gum spectra is slightly lesser than the spectra with 0.1 g of salt. The slight increase in the crystallinity after the addition of salt may be due to the reordering/rearrangement of the polymer segment to incorporate the salt dopant. However the degree of crystallinity begins to decrease with the further addition of salt above 0.1 g. The film GT:LN-1 g:0.4 g shows the least crystallinity value of 25.23% making it with the highest amorphous nature. The increase in the

Table 1. List of samples and their compositions.

SAMPLE CODE	GT	LN
P	1 g	-
A	1 g	0.1 g
B	1 g	0.2 g
C	1 g	0.3 g
D	1 g	0.4 g

amorphousness as the salt content is raised, is directly proportional to the conductivity of the film. This is because the movement of the polymer chains is enhanced in the amorphous state as they are entangled and irregular with lower density and molecular packing. Contrarily the high density molecular packing of the polymer chains in the crystalline region does not aid in the mobility of the polymer chains.[18,19] Thus, the highest amorphous film having a high ionic diffusivity produces the maximum ionic conductivity. The shift in the overall peak and the absence of diffraction peak pertaining to $LiNO_3$ indicates that the salt is completely dissociated within the host polymer matrix.[20]

3.2. FTIR analysis

The interactions among atoms and ions in an electrolyte system can induce changes in the vibrational modes of the molecules, which can be analyzed using FTIR. Figure 3 shows the FTIR spectrum of pure GT and GT-

$LiNO_3$ complexes of various compositions in the range 400–4000 cm^{-1}. The major absorbance bands of gum tragacanth present in the spectrum were observed at 3332, 2937, 1720, 1600, 1244, 1145, 1036, and 988 cm^{-1}. The stretching vibrations of the hydroxyl (-OH) groups appear as a broad band at 3332 cm^{-1} and shifts to larger wavenumber with the addition of salt.[10,21]

The absorption band at 2937 cm^{-1} corresponds to the asymmetrical stretching vibrations of the methylene ($-CH_2$) group. The peak at 1720 cm^{-1} could be assigned to the carbonyl stretching vibrations in carboxylic acids (C = O stretching of −COOH) while the strong band at 1600 cm^{-1} can be assigned to the characteristic asymmetrical stretch of carboxylate anion form of D-galacturonic acid present in tragacanth gum (C = O stretching of −COO$^-$). As the salt concentration increases these peaks shifts to 1727 and 1623 cm^{-1} for the highest conducting film.[16,17,20] The C–O stretching vibrations of polyols, ether, and alcoholic groups are observed at 1244, 1145, and 1036 cm^{-1}.[21] The shift observed in the above peaks when compared to pure GT indicates the formation of complex polymer electrolyte.

The peaks ranging between 800 and 1200 cm^{-1} are known to be the fingerprint region of carbohydrates and can be attributed to C–O, C–C, ring structures, and deformation vibrations of CH_2 groups.[16,17,22]

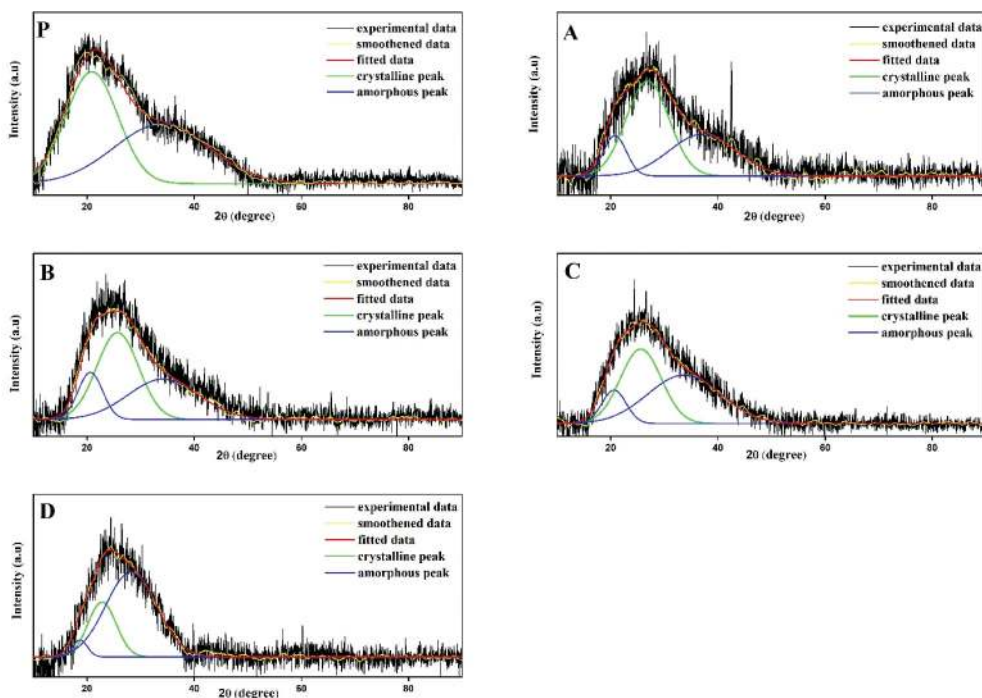**Figure 1.** Photograph of GT:LN-1 g:0.4 g SPE.

Figure 2. Deconvoluted x-ray diffraction patterns for the different GT:LN polymer complexes.

A small peak observed at 1373 cm^{-1} for pure GT intensifies and shifts to a lower wavenumber of 1336 cm^{-1} for the film with the maximum salt concentration. This peak corresponds to the asymmetric stretching mode of NO$_3^-$ ions which was due to the addition of LiNO$_3$. Thus, with the increase in LiNO$_3$ salt to the gum this strong peak broadens and intensifies hence proving the complexation of the salt with the host polymer matrix.[23,24]

Due to the high complexation of the nitrate ions with the polymer matrix the band in the region 1300–1500 cm^{-1} is deconvoluted to study the free ions and contact ions percentage in the films. Baseline correction was done prior to deconvolution. It can be seen from Figure 4 that the deconvolution of the band gives rise to three peaks, in which the peak in the region 1350 – 1380 cm^{-1} corresponds to the free ions and the peaks around 1320–1340 cm^{-1} and 1410–1420 cm^{-1} are assigned to the contact ions.[25–27]

The free ions percentage can be calculated by the following equation and the values are tabulated in Table 3,

$$Free\ ions\ \% = \frac{A_f}{A_f + A_c} \times 100\% \qquad (2)$$

where A_f and A_c correspond to the area under the free ion and contact ions peaks.

It can be observed that the fraction of free ion percentage gradually increases as the salt content increases. Hence, the ionic conductivity is increased with the addition of salt. Accordingly, the contact ions percentage also reaches a minimum with the addition of salt. The sample GT:LN- 0.1 g:0.4 g exhibits the highest free ions percentage and hence the maximum conductivity.

A correlation between the shift in frequency and force constant is established using the following equation:[28,29]

$$\bar{v} = \frac{1}{2\pi c} \sqrt{\frac{k}{\mu}} \qquad (3)$$

where is wavenumber in cm^{-1}, c is the velocity of light (3×10^{10} cm/s), k is the force constant in cm^{-1} and μ is the reduced mass, which is given by the following expression, $\mu = M_1M_2/(M_1 + M_2)$ where M_1 and M_2 are atomic weights of the two atoms, respectively.

The force constant values for NO$_3^-$ ions stretching are calculated from equation 3 and tabulated in Table 4. It can be noted from the table that the force constant

Table 2. The degree of crystallinity from the deconvoluted XRD spectra.

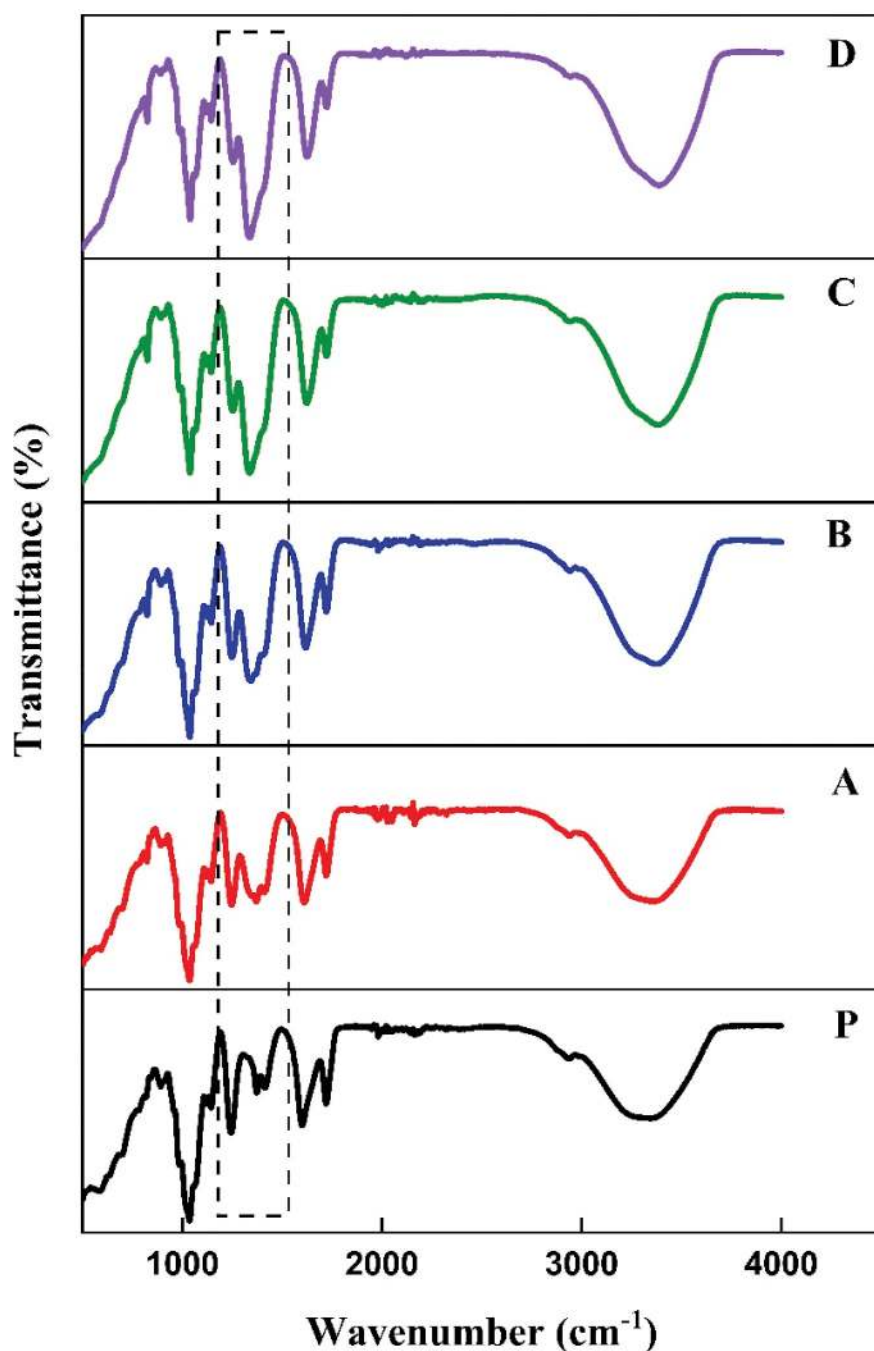| Sample	Degree of Crystallinity (%)
P	50.67
A	52.40
B	47.58
C	41.28
D	25.23

Figure 3. FTIR Spectra for the various GT:LN polymer electrolytes.

values decrease with the addition of salt. This can be due to the interaction of the nitrate ions with the host polymer matrix hence confirming the complexation of the salt.[30,31]

3.3. Conductivity studies

The AC impedance technique is the most eminent and effective tool for characterizing the electrical properties of the materials. The impedance spectra of GT:LN polymer complex are shown in the Figure 5. Two well-defined regions are observed in the Figure. The high-frequency semi-circle is related to the ionic conduction due to the parallel combination of bulk resistance (R_b) and bulk capacitance and a low-frequency spur represents the formation of double-layer capacitance at the electrode/electrolyte interface due to diffusion.[32] The value of R_b is determined from the intercept of the semicircle and spur. The R_b value decreases with

increase in the salt concentration and this may be due to the increase in mobile charge carriers.[33] The ionic conductivity of the sample was calculated using the following formula:

$$\sigma = \frac{t}{R_b A} \quad (4)$$

where σ is the conductivity, t is the thickness of the electrolyte, R_b is the bulk resistance and A is the contact area of the electrodes. The room temperature ionic conductivities calculated for all the prepared polymer electrolytes are tabulated in Table 5. The highest conductivity is found to be 8.28×10^{-3} Scm^{-1} for the ratio of GT:LN-1 g:0.4 g (sample D).

3.4. Temperature dependent ionic conductivity

The temperature-dependent conductivity for the GT:LN samples over the temperature range 308–343 K are shown in Figure 6. The conductivity of all samples increases linearly with increase in temperature which obeys Arrhenius relationship:

$$\sigma = A e \left(\frac{-E_a}{kT} \right) \quad (5)$$

where A is a constant that is proportional to the amount of charge carriers, E_a is the activation energy, k is the Boltzmann constant, and T is the temperature in kelvin. The increase in ionic conductivity with temperature can be described by free volume model[34] due to the increase in mobility of ions which leads to the increase in segmental motion of the polymer chain.

The increase in temperature produces high vibrational energy in the polymer segments thus creating a hydrostatic pressure by the neighboring atoms.[35] By overcoming this hydrostatic pressure by the atoms, a small amount of space is developed around its own volume, and thus the segmental motion of the polymer chain and dissociation of the salt increases resulting in the decrease in bulk resistance (R_b) value.[36]

The activation energy is calculated for all the samples by linear fit of Arrhenius plot. The value of E_a decreases with increase in salt concentration. This may be due to the increase in amorphous nature of the polymer salt complex which enhances the ionic motion of charge carriers in the polymer electrolyte. For the highest conductivity sample the value of E_a is found to be 0.21 eV.
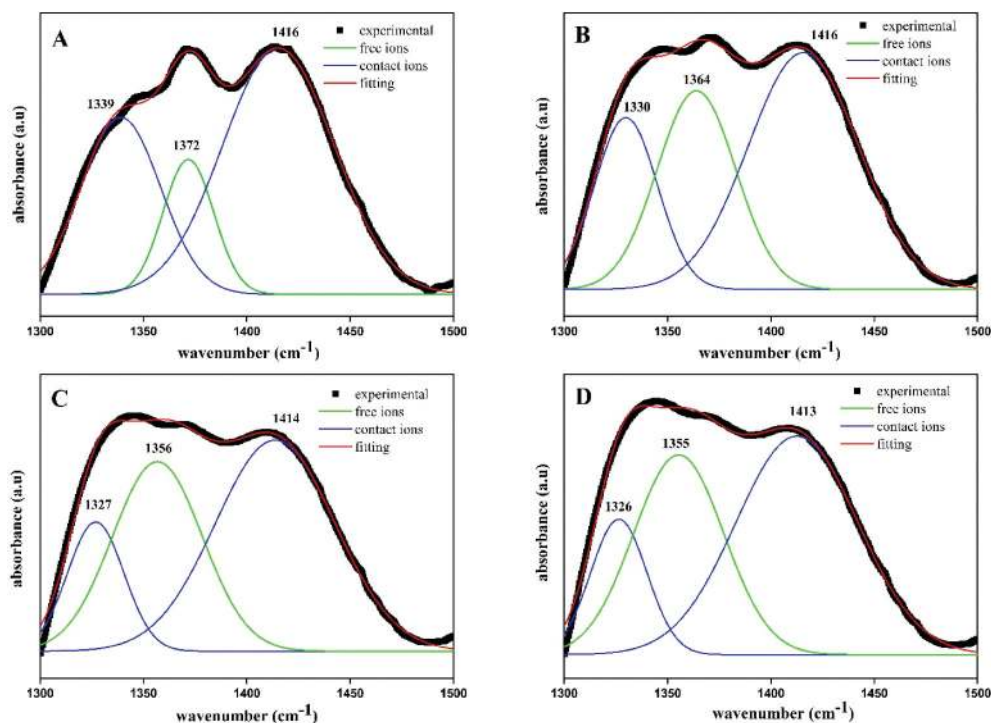
Table 3. Free ions and contact ions percentage for the GT:LN system.

Sample	Free ions (%)	Contact ions (%)
A	14.19	85.80
B	29.68	70.31
C	34.34	65.65
D	35.48	64.51

Figure 4. Deconvoluted FTIR spectra in the region 1300–1500 cm^{-1}.

Table 4. FTIR mode of NO_3^- ions stretching vibrations in GT:LN polymer complexes.

Sample	NO_3^- ions stretching vibrations	
	Wavenumber/cm^{-1}	Force constant/Ncm^{-1}
P(pure)	1374	8.24
A	1370	8.21
B	1343	7.88
C	1337	7.81
D	1336	7.80

3.5. Conductance spectra

Figure 7 shows the variation of $log\ \sigma$ as a function of frequency. It is observed from the figure that conduction spectra consist of two regions, low-frequency-dispersive region and intermediate-frequency-independent plateau region. The low-frequency-dispersive region is attributed to the space charge polarization at the blocking electrode.[37] The extrapolation of the frequency-independent plateau region to the $log\ \sigma$ axis gives the dc conductivity of the polymer electrolyte.

It is observed from Figure 8 that the value of dc conductivity increases and activation energy decreases with the addition of salt.

3.6. Dielectric studies

The complex dielectric of a system is defined by

$$\varepsilon^* = \varepsilon_r - j\varepsilon_i \qquad (6)$$

where ε_r is the dielectric constant and ε_i is the dielectric loss. ε_r and ε_i were calculated using the following equations:

$$\varepsilon_r = \frac{z_i}{\omega c_0 \left(z_r^2 + z_i^2\right)} \qquad (7)$$

$$\varepsilon_i = \frac{z_r}{\omega C_0 \left(z_r^2 + z_i^2\right)} \qquad (8)$$

Here $C_0 = \frac{\varepsilon_0 A}{t}$ and $\omega = 2\pi f$

where ε_0 is the permittivity of the free space, f is the frequency, z_i and z_r are the imaginary and real part of impedance. The dielectric behavior of the polymer electrolyte is used to determine the polarization effects due to the blocking electrodes. ε_r is the measure of amount of charge stored in the material and ε_i is the measure of loss in energy due to the movement of ions when electric field reverses.[38] The variation of dielectric constant and dielectric loss as a function of frequency is shown in Figures 9 and 10. The relaxation peak observed around 4 KHz for sample D (GT:LN-1 g:0.4 g) in the dielectric constant curve is a fast relaxation process that can be attributed to the polymer segmental dielectric relaxation (α relaxation).[39,40] The broad nature of the peak may be due to the different mechanisms associated with local molecular motions.[41]

The graph of ε_i is similar to ε_r. When the polarity of AC signal is reversed, the movement of the ions decelerates, stops and it accelerates in the opposite
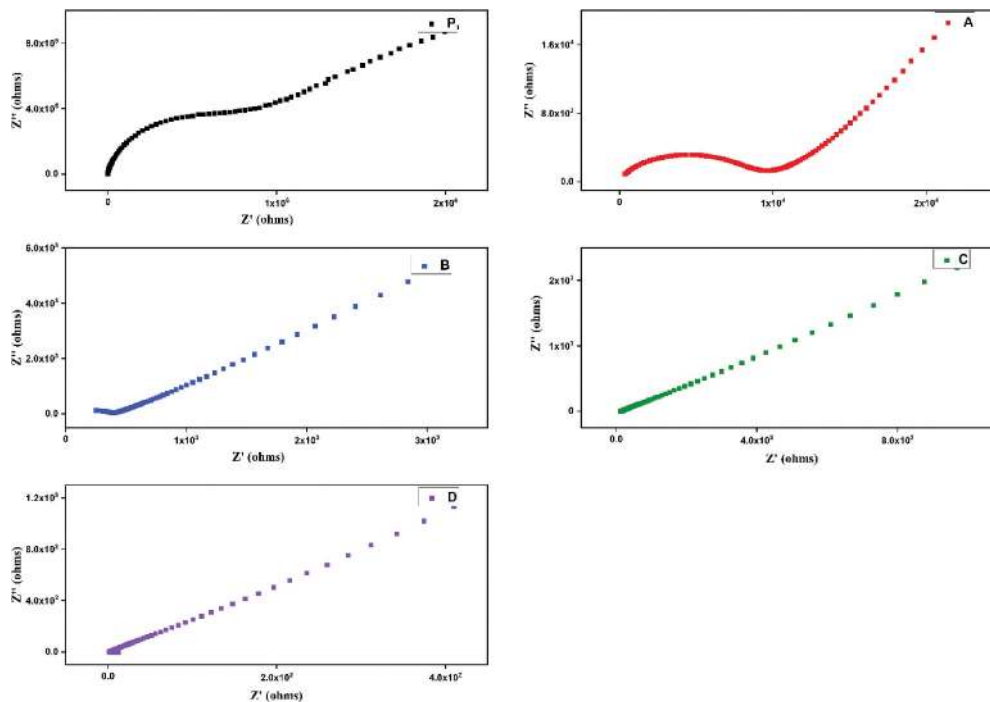

Figure 5. Cole-Cole plots for the various GT:LN polymer electrolytes.

Table 5. Bulk resistance and ionic conductivity values for the various GT:LN polymer complexes.

Sample	Bulk resistance R_b (Ω)	Ionic conductivity σ (Scm^{-1})
P	1.06×10^6	2.10×10^{-8}
A	9.76×10^3	1.89×10^{-6}
B	3.93×10^2	5.69×10^{-5}
C	14.10	1.03×10^{-3}
D	1.755	8.28×10^{-3}

direction. Therefore, energy loss is observed due to the dissipation of heat through internal friction.[42] The value of rises sharply at low frequency and decreases with increase in frequency. The high value of dielectric constant is due to the space charge polarization effects which may be attributed to the accumulation of charges at the electrode–electrolyte interface.[43] The decrease in value of at high frequency is due to the periodic reversal of the electric field occurs so fast such that charge carriers are hard to orient themselves in the direction of field.[44] The decrease in value of ε_i and ε_r confirms the non-Debye behavior of polymer electrolyte system.[45]
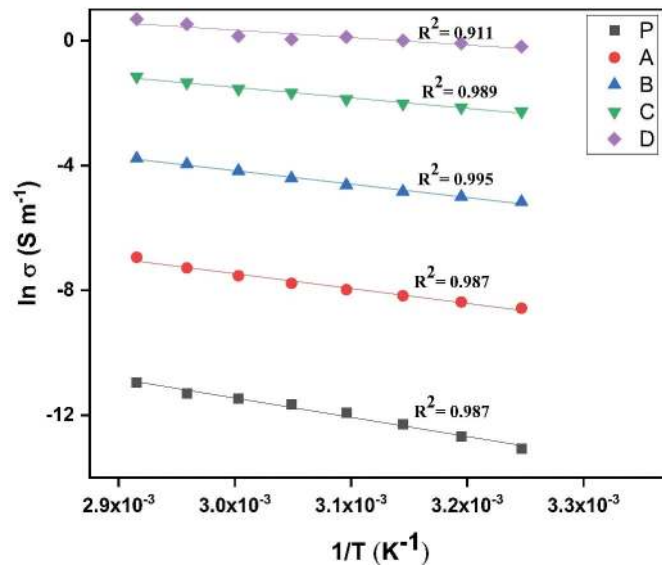
Figure 6. Temperature dependent conductivity for the various GT:LN polymer electrolytes.
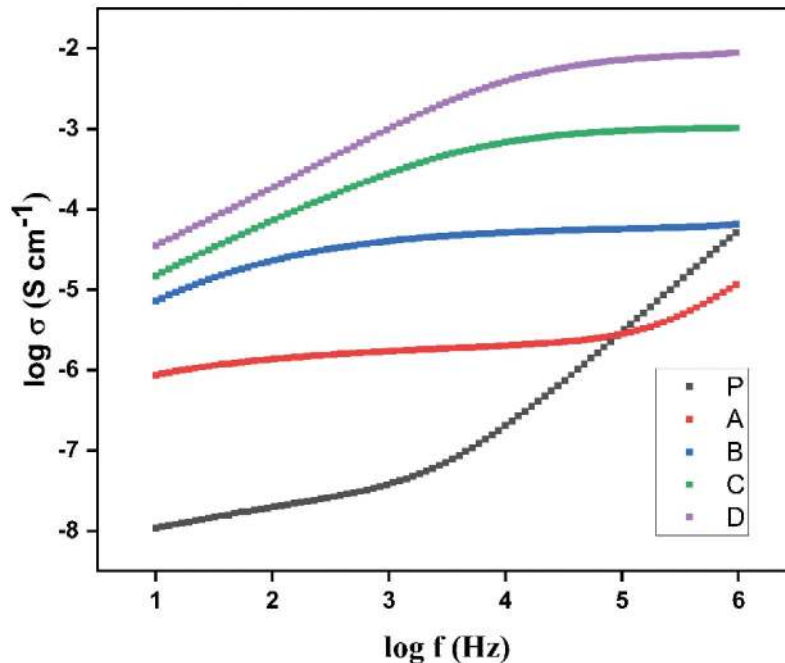
Figure 7. Conductance Spectra for the different GT:LN polymer electrolytes.

3.7. Transference number measurement

The total ionic and electronic transference number of the polymer electrolyte GT:LN-1 g:0.4 g system was calculated using Wagner's polarization technique.[46] On applying a dc potential of 1.5 V across the sample with blocking electrode the dc current is monitored as a function of time. The time dependence of dc polarization current at 303 K is shown in Figure 11.

The transference number were calculated using the following equation:

$$t_{ion} = (I_i - I_f)/I_i \quad (9)$$
$$t_{elec} = I_f/I_i \quad (10)$$

where I_i is the initial current and I_f is the final residual current. The total ionic transference number was found to be 0.989. This result suggests that the charge transport in the polymer electrolyte system is predominantly due to Li^+ ions that are smaller in ionic size and a negligible contribution from the electrons to the total current.

3.8. Electrochemical stability

Electrochemical stability is an essential parameter that establishes the maximum potential limits possible for device application.[23] Electrochemical stability defines a reliable potential window for the polymer electrolyte which was studied by linear sweep voltammetry and the corresponding voltammogram is shown in Figure 12. The polymer electrolyte was sandwiched between stainless steel electrodes and a potential in the range 0–4 V was applied at a scan rate of 100 mV/s. It is evident from the figure that the current onset begins at 3.4 V. The onset of current is associated with the breakdown voltage of the electrolyte.[47] The electrochemical potential

of 3.4 V is suitable to be used in the application of lithium polymer battery.

3.9. Thermogravimetric analysis

Thermogravimetric analysis (TGA) is an effective tool to study the thermal stability of the polymer electrolytes. The samples were heated at the rate of 20°C/min from 30°C to 600°C under constant nitrogen flow. The thermogram of pure GT and the complex of GT+LN (GT:LN-1 g:0.4 g) are shown in Figure 13. As seen from the figure the polymer electrolyte undergoes a three-step thermal degradation. The first-step weight loss occurs below 240°C which is due to the evaporation of the entrapped moisture within the films.[48] The actual degradation of the sample occurs around the second and third step at 240°C and 300°C. These two-step weight losses can be due to the loss of the hydroxyl groups and carbon dioxide from the gum.[16,48] It can also be associated with the heterogenous nature of the gum consisting of the water soluble and insoluble fractions.[49] The residue at 600°C is about 36.4% and 38.4% for pure GT and GT+LN. The thermograms of pure GT and GT+LN are similar, with the thermal degradation occurring around the same temperature range making it suitable for practical application.

4. Conclusion

A new solid polymer electrolyte based on Gum Tragacanth and Lithium Nitrate has been prepared and characterized by XRD, FTIR, Impedance spectroscopy and LSV. XRD and FTIR confirm the complexation of
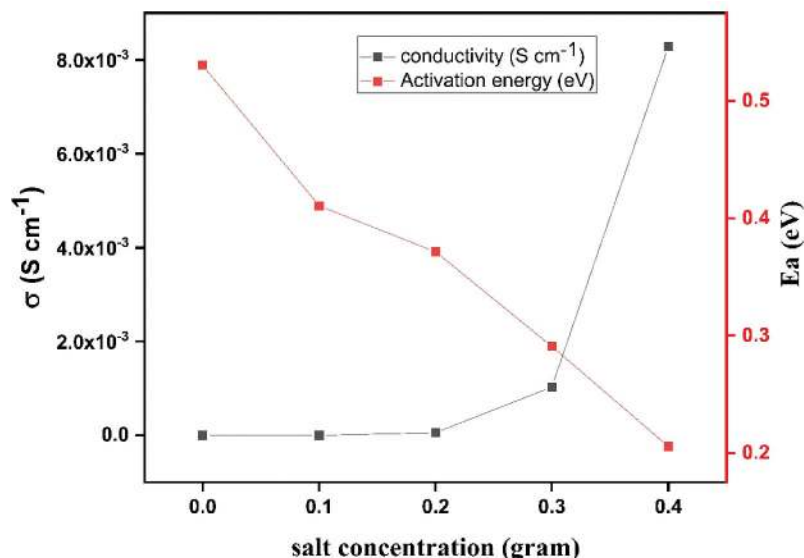

Figure 8. Ionic conductivity and activation energy for the different GT:LN polymer electrolytes.
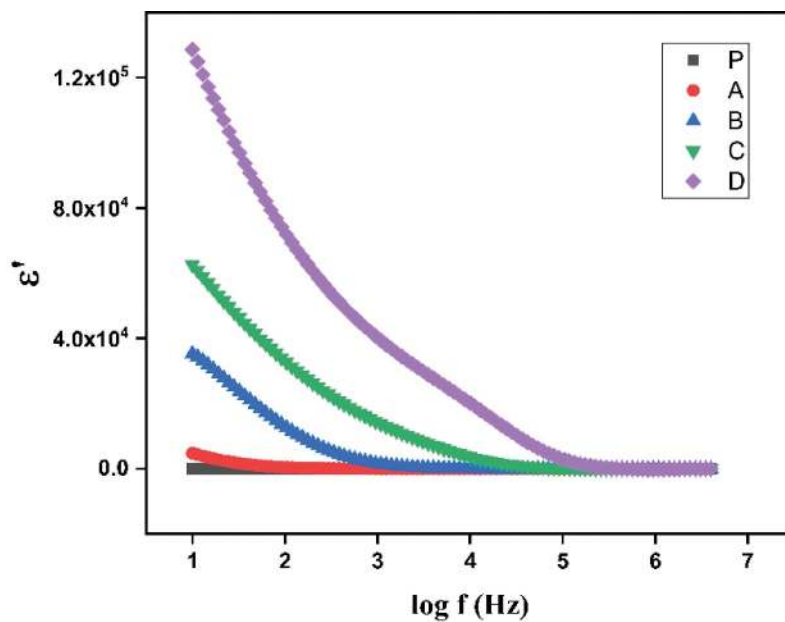
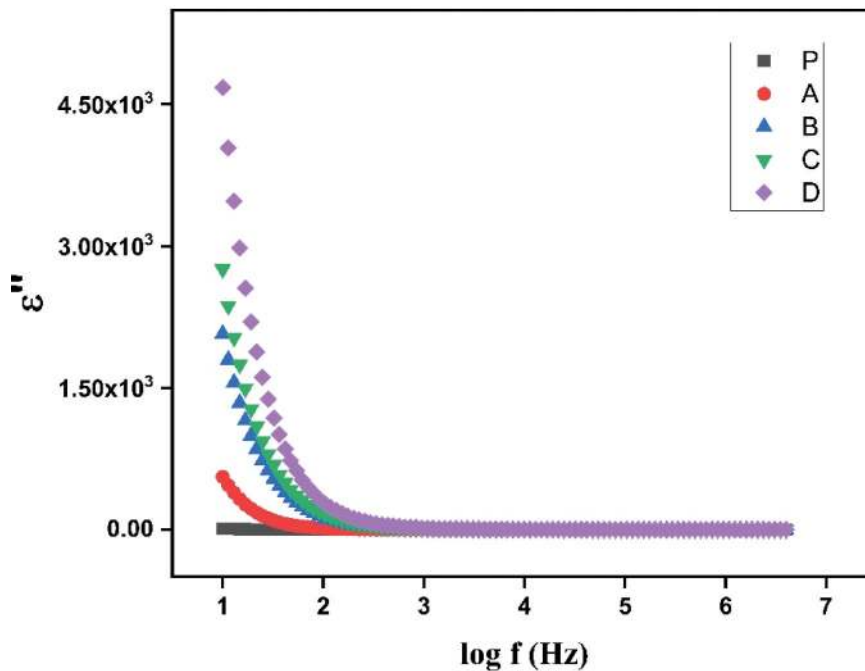**Figure 9.** Dielectric constant for the different GT:LN polymer electrolytes.

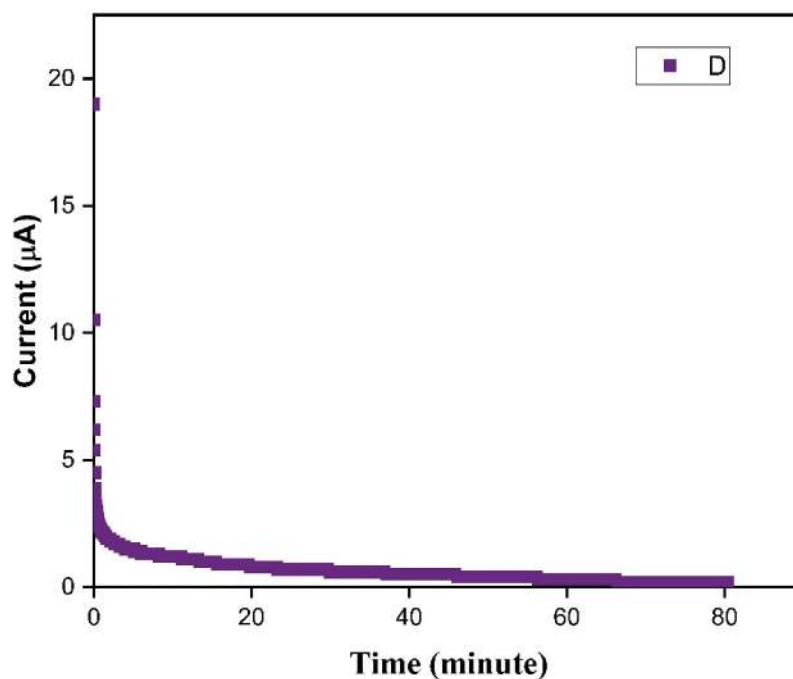**Figure 10.** Dielectric loss for the different GT:LN polymer electrolytes.

Figure 11. Polarization current verus time plot for the sample GT:LN-1 g:0.4 g.

the salt with the polymer matrix. The highest ionic conductivity of 8.28×10^{-3} Scm^{-1} was obtained for the composition GT:LN-1 g:0.4 g. The temperature-dependent conductivity exhibited Arrhenius behavior while the dielectric studies confirm the non-Debye behavior of the electrolytes. The electrochemical stability of
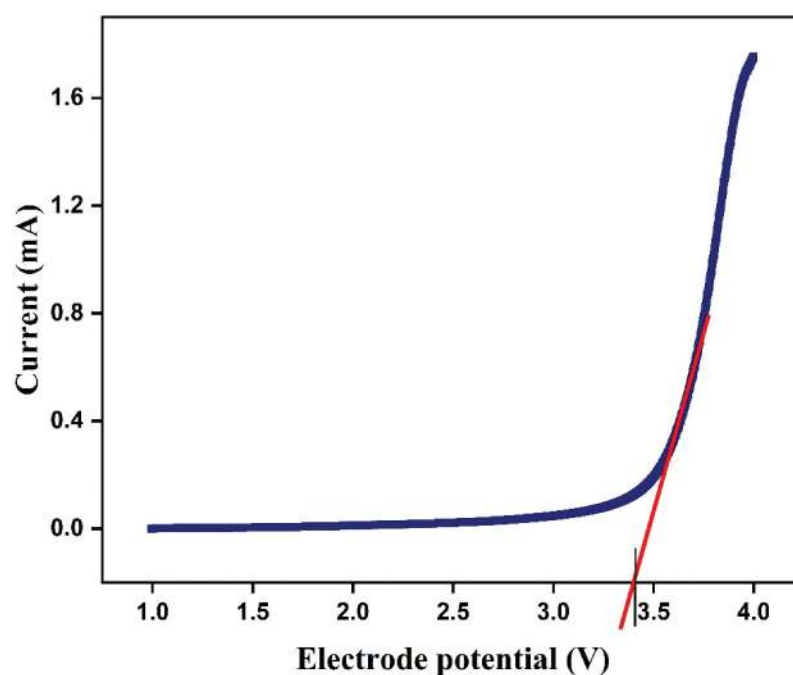

Figure 12. Linear sweep voltammogram for the highest conducting film GT:LN-1 g:0.4 g.
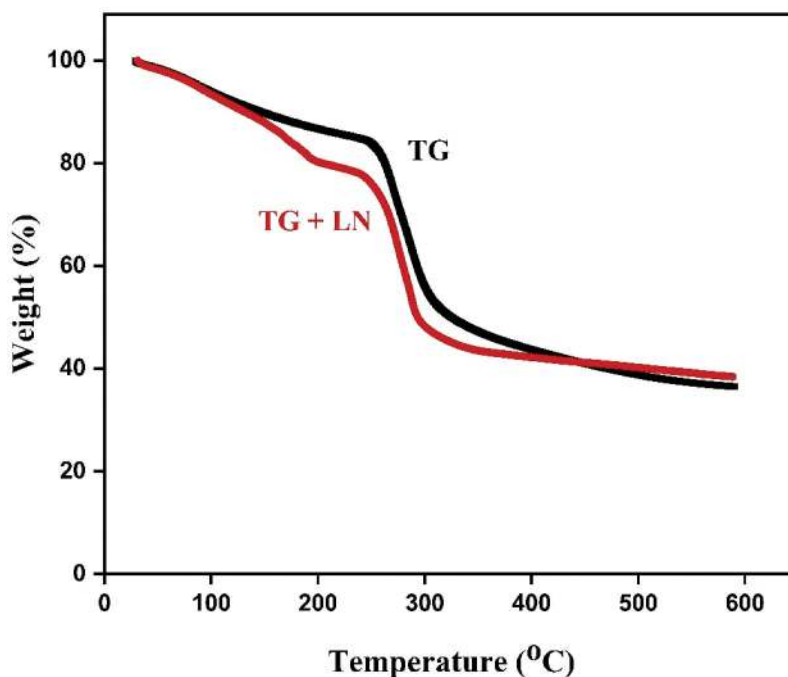
Figure 13. Thermogram of Pure GT and GT+LN (GT:LN-1 g:0.4 g) complex.

3.4 V and thermal stability up to 240°C obtained from Linear sweep voltammetry and thermogravimetric analysis makes the polymer electrolyte suitable for practical applications.

Availability of data

The data that support the findings of this study are available from the corresponding author, Dr. S. Karthikeyan, upon reasonable request.

Acknowledgment

Disclosure statement

The authors declare that they have no conflict of interest.

Funding

Notes on contributors

Jenova, I, received her M.Sc.in Physics from Madras Christian College, Chennai and registered as a research scholar in the Department of Physics of the same college affiliated to the University of Madras. Her research interests include polymer electrolytes and batteries

Venkatesh. K, is a research scholar in the Department of Physics, Madras Christian College, Chennai. He completed his Master Degree in Physics at Madras Christian College, Chennai. His research interest is in the field of solid state Ionics.

Dr. Karthikeyan S, is working as Assistant Professor in the Department of Physics, Madras Christian College, Tambaram, Tamilnadu. He received his M. Sc. in Physics from Alagappa University, Karaikudi and his PhD from University of Twente, The Netherlands. He has Post-Doctoral experience from Chalmers University of Technology, Sweden. Previously he worked at Kalasalingam University, Srivilliputhur, VIT University, Vellore and Ramco Institute of Technology, Rajapalayam. He has published more than 35 papers in the leading journals. He is a life member of Indian Physics Association. His research interests include membrane studies, fuel cells, batteries and sensors. He has guided 4 PhD students and currently he is guiding 3 PhD research scholars.

Dr. Madeswaran S is an Assistant Professor (Sr.) of physics at Centre for Functional Materials (CFM) Vellore Institute of Technology. He obtained his Ph.D. degree from Anna University. His Ph.D. research work is on the "Growth and characterization of ferroelectric single crystals and thin films". After his Ph.D., he joined the National Institute for Materials Science (NIMS), Tsukuba, Japan as a Postdoc researcher. He worked (2 years) there on the fabrication of Al_2O_3 single crystalline nano-film (~10 nm) for the application of MIM emitters. He then moved to Tokyo University of Science (TUS), Japan and investigated (4 years) hard magnetic (NdFeB) thin films, which are widely used in MEMS applications. He then joined VIT in 2011 and is involved in teaching and research. His major research areas are ferroelectric/magnetic, energy and NLO materials. He has to his credit several research papers published in internationally reputed journals.

He is currently guiding five research students. He is a life member of Magnetic Society of India and Indian Association for crystal growth.

Dr. Arivanandhan. M, is an Associate Professor at Centre for Nanoscience and Technology, Anna University, India. He graduated from Alagappa University, India and he was a postdoctoral fellow at IMR, Tohoku University, Japan. He has worked as Assistant Professor at RIE, Shizuoka University, Japan. He has more than 15 years of research experience in Crystal Engineering and Nanotechnology. His research interests include alloy semiconductors, Nanoenergy materials, Graphene based nanocomposites, solar cells and thermoelectrics. He has published 175 papers in International Journals and presented more than 270 papers in National/International conferences. He holds three patent. He has received several awards including Young Achiever Award and Young Scientist Award.

Dr. Joice Sheeba. D, is currently an Assistant Professor in Physics at Madras Christian College, Chennai. She is actively involved in research in the field of polymer electrolyte. She has guided two M.Phil. students and several M.Sc. students.

ORCID

Karthikeyan S 🆔 http://orcid.org/0000-0002-7674-7157

References

[1] Bruce, P. G.;. *Solid State Electrochemistry*; Cambridge University Press, 1995.

[2] Harun, N. I.; Ali, R. M.; Ali, A. M. M.; Yahyap, M. Z. A. Conductivity Studies on Cellulose Acetate–Ammonium Tetrafluoroborate Based Polymer Electrolytes. *Mater. Res. Innovations.* 2011, *15*(2), 168–172. DOI: 10.1179/143307511X13031890748858.

[3] Leones, R.; Sentanin, F.; Rodrigues, L. C.; Marrucho, I. M.; Esperança, J. M. S. S.; Pawlicka, A.; Silva, M. M. Investigation of Polymer Electrolytes Based on Agar and Ionic Liquids. *Express Polym. Lett.* 2012, *6* (12), 1007–1016. DOI: 10.3144/expresspolymlett.2012.106.

[4] Osman, Z.; Arof, A. K. FTIR Studies of Chitosan Acetate Based Polymer Electrolytes. *Electrochim. Acta.* 2003, *48*, 993–999. DOI: 10.1016/S0013-4686(02)00812-5.

[5] Karthikeyan, S.; Selvasekarapandian, S.; Premalatha, M.; Monisha, S.; Boopathi, G.; Aristatil, G.; Arun, A.; Madeswaran, S. Proton-conducting I-Carrageenan-based Biopolymer Electrolyte for Fuel Cell Application S. *Ionics.* 2017, *23*, 2775–2780. DOI: 10.1007/s11581-016-1901-0.

[6] Dos Santos, M. A.; Grenha, A. Polysaccharide Nanoparticles for Protein and Peptide Delivery: Exploring Less-Known Materials. *Adv Protein Chem Struct Biol.* 2015, *98*, 223–261.

[7] Beach, D. C.;. History, Production, and Uses of Tragacanth, Chapter 7. In *Natural Plant Hydrocolloids*, 1954; pp 38–44.

[8] Khajavi, R.; Mossavi, S. H.; Kiumarsi, A.; Rashidi, A. Gum Tragacanth from *Astragalus Gummifer* Species: Effects of Influencing Factors on Mechanical Properties of Fibers. *J. Appl. Sci.* 2007, *7*(19), 2861–2865. DOI: 10.3923/jas.2007.2861.2865.

[9] Gorji, S. G.; Gorji, E. G.; Mohammadifar, M. A.; Zargaraan, A. Complexation of Sodium Caseinate with Gum Tragacanth: Effectof Various Species and Rheology of Coacervates. *Int. J. Biol. Macromol.* 2014, *67*, 503–511. DOI: 10.1016/j.ijbiomac.2014.02.037.

[10] Zare, E. N.; Makvandi, P.; Tay, F. R. Recent Progress in the Industrial and Biomedical Applications of Tragacanth Gum: A Review. *Carbohydr. Polym.* 2019, *212*, 450–467. DOI: 10.1016/j.carbpol.2019.02.076.

[11] Arockia Mary, I.; Selvanayagam, S.; Selvasekarapandian, S.; Srikumar, S. R.; Ponraj, T.; Moniha, V. Lithium Ion Conducting Membrane Based on K-carrageenan Complexed with Lithium Bromide and Its Electrochemical Applications. *Ionics.* 2019, *25*, 5839–5855. DOI: 10.1007/s11581-019-03150-x.

[12] Yahya, M. Z. A.; Arof, A. K. Effect of Oleic Acid Plasticizer on Chitosan–lithium Acetate Solid Polymer Electrolytes. *Eur. Polym. J.* 2003, *39*, 897–902. DOI: 10.1016/S0014-3057(02)00355-5.

[13] Teoh, K. H.; Chin-Shen Lim, R. S. Lithium Ion Conduction in Corn Starch Based Solid Polymer Electrolytes. *Measurement.* 2014, *48*, 87–95. DOI: 10.1016/j.measurement.2013.10.040.

[14] Perumal, P.; Christopher Selvin, P.; Selvasekarapandian, S.; Sivaraj, P. Structural and Electrical Properties of Bio-polymer Pectin with LiClO4 Solid Electrolytes for Lithium Ion Polymer Batteries. *Mater. Today Proc.* 2019, *8*, 196–202.

[15] Abidin, S. Z. Z.; Ali, A. M. M.; Hassan, O. H.; Yahya, M. Z. A. Electrochemical Studies on Cellulose Acetate-LiBOB Polymer Gel Electrolytes. *Int. J. Electrochem. Sci.* 2013, *8*, 7320–7326.

[16] Singh, B.; Sharma, V. Influence of Polymer Network Parameters of Tragacanth Gum-based pH Responsive Hydrogels on Drug Delivery. *Carbohydr. Polym.* 2014, *101*, 928–940. DOI: 10.1016/j.carbpol.2013.10.022.

[17] Kurt, A.;. Physicochemical, Rheological and Structural Characteristics of Alcohol Precipitated Fraction of Gum Tragacanth. *Food and health.* 2018, *4*(3), 183–193. DOI: 10.3153/FH18019.

[18] Woo, H. J.; Liew, C.-W.; Majid, S. R.; Arof, A. K. Poly(ε-caprolactone)-based Polymer Electrolyte for Electrical Double-layer Capacitors. *High Perform Polym.* 2014, *26* (6), 637–640. DOI: 10.1177/0954008314542168.

[19] Brza, M. A.; Aziz, S. B.; Anuar, H.; Ali, F.; Hamsan, M. H.; Kadir, M. F. Z.; Abdulwahid, R. T. Metal Framework as a Novel Approach for the Fabrication of Electric Double Layer Capacitor Device with High Energy Density Using Plasticized Poly(vinyl Alcohol): Ammonium Thiocyanate Based Polymer Electrolyte. *Arabian J. Chem.* 2020, *13*, 7247–7263. DOI: 10.1016/j.arabjc.2020.08.006.

[20] Rajeswari, N.; Selvasekarapandian, S.; Prabu, M.; Karthikeyan, S.; Sanjeeviraja, C. Lithium Ion Conducting Solid Polymer Blend Electrolyte Based on Bio-degradable Polymers. *Bull. Mater. Sci.* 2013, *36*, 333–339. DOI: 10.1007/s12034-013-0463-2.

[21] Kora, A. J.; Arunachalam, J. Green Fabrication of Silver Nanoparticles by GumTragacanth (Astragalus Gummifer): A Dual Functional Reductant and Stabilizer. *J. Nanomater.* 2012. DOI: 10.1155/2012/869765.

[22] Nep, E. I.; Conway, B. R. Physicochemical Charac-terization of Grewia Polysaccharide Gum: Effect of Dry-ing Method. *Carbohydr. Polym.* 2011, *84* (1), 446–453. DOI: 10.1016/j.carbpol.2010.12.005.

[23] Jinisha, B.; Anilkumar, K. M.; Manoj, M.; Pradeep, V. S.; Jayalekshmi, S. Development of a Novel Type of Solid Polymer Electrolyte for Solid State Lithium Battery Applications Based on Lithium Enriched Poly (Ethylene Oxide) (Peo)/poly (Vinyl Pyrrolidone) (PVP) Blend Polymer. *Electrochim. Acta.* 2017, *235*, 210–222. DOI: 10.1016/j.electacta.2017.03.118.

[24] Monisha, S.; Mathavan, T.; Selvasekarapandian, S.; Milton Franklin Benial, A.; Prema Latha, M. Preparation and Characterization of Cellulose Acetate and Lithium Nitrate for Advanced Electrochemical Devices. *Ionics.* 2016.

[25] Arya, A.; Sharma, A. L. Dielectric Relaxations and Transport Properties Parameter Analysis of Novel Blended Solid Polymer Electrolyte for Sodium Ion Rechargeable Batteries. *J. Mater. Sci.* 2019, *54*, 7131–7155. DOI: 10.1007/s10853-019-03381-3.

[26] Hafizaa, M. N.; Isa, M. I. N. Correlation between Structural, Ion Transport and Ionic Conductivity of Plasticized 2-hydroxyethyl Cellulose Based Solid Biopolymer Electrolyte. *J. Membr. Sci.* 2020, *597*, 117–176. DOI: 10.1016/j.memsci.2019.117176.

[27] Aziz, S. B.; Dannoun, E. M. A.; Hamsan, M. H.; Ghareeb, H. O.; Nofal, M. M.; Karim, W. O.; Asnawi, A. S. F. M.; Hadi, J. M.; Kadir, M. F. Z. A. A Polymer Blend Electrolyte Based on CS with Enhanced Ion Transport and Electrochemical Properties for Electrical Double Layer Capacitor Applications. *Polymers.* 2021, *13*, 930. DOI: 10.3390/polym13060930.

[28] Stuart, B.;. *Infrared Spectroscopy: Fundamentals and Applications*; Wiley, 2004; pp 8.

[29] Pavia, D. L.; Lampman, G. M.; Kriz, G. S. *Introduction to Spectroscopy*;third; Harcourt College Publishers: New York, 2001; pp 19.

[30] Ravi, M.; Bhavani, S.; Kiran Kumar, K.; Narasimaha Rao, V. V. R. Investigations on Electrical Properties of PVP:KIO$_4$ Polymer Electrolyte Films. *Solid State Sci.* 2013, *19*, 85–93. DOI: 10.1016/j.solidstatesciences.2013.02.006.

[31] Abdelaziz, M.; Ghannam, M. M. Influence of Titanium Chloride Addition on the Optical and Dielectric Properties of PVA Films. *Physica B Condensed Matter* 2010, *405*, 958–964. DOI: 10.1016/j.physb.2009.10.030.

[32] Ravi, M.; Pavani, Y.; Kiran Kumar, K.; Bhavani, S.; Sharma, A. K.; Narasimha Rao, V. V. R. Studies on Electrical and Dielectric Properties of PVP:KBrO4 Complexed Polymer Electrolyte Films. *Mater. Chem. Phys.* 2011, *130*, 442–448. DOI: 10.1016/j.matchemphys.2011.07.006.

[33] Aziz, S. B.; Brevik, I.; Hamsan, M. H.; Brza, M. A.; Nofal, M. M.; Abdullah, A. M.; Rostam, S.; Al-Zangana, S.; Muzakir, S. K.; Kadir, M. F. Z. Compatible Solid Polymer Electrolyte Based on Methyl Cellulose for Energy Storage Application: Structural, Electrical, and Electrochemical Properties. *Polymers.* 2020, *12*(10), 2257. DOI: 10.3390/polym12102257.

[34] Pillai, P. K. C.; Khurana, P.; Trilateral, A. Dielectric Studies of Poly(methyl Methacrylate)/polystyrene Double Layer System. *J. Mater. Sci. Lett.* 1986, *5*, 629. DOI: 10.1007/BF01731531.

[35] Sundaramahalingam, K.; Vanitha, D.; Nallamuthu, N.; Manikandan, A.; Muthuvinayagam, M. Electrical Properties of Lithium Bromide Poly Ethylene Oxide/poly Vinyl Pyrrolidone Polymer Blend Electrolyte. *Physica B: Condens. Matter* 2019, *553*, 120–126. DOI: 10.1016/j.physb.2018.10.040.

[36] Sampathkumar, L.; Selvin, P. C.; Selvasekarapandian, S.; Perumal, P.; Chitra, R.; Muthukrishnan, M. Synthesis and Characterization of Biopolymer Electrolyte Based on Tamarind Seed Polysaccharide, Lithium Perchlorate and Ethylene Carbonate for Electrochemical Applications. *Ionics.* 2019, *25*, 1067–1082. DOI: 10.1007/s11581-019-02857-1.

[37] Kingslin Mary Genova, F.; Selvasekarapandian, S.; Karthikeyan, S.; Vijaya, N.; Sivadevi, S.; Sanjeeviraja, C. Lithium Ion-Conducting Blend Polymer Electrolyte Based on PVA-PAN Doped with Lithium Nitrate. *Polym. Plast. Technol. Eng..* 2016, *55* (1), 25–35. DOI: 10.1080/03602559.2015.1050523.

[38] Navaratnam, S.; Sanusi, A.; Ahmad, A. H.; Ramesh, S.; Ramesh, K.; Othman, N. Conductivity Studies of Biopolymer Electrolyte Based on Potato Starch/Chitosan Blend Doped with LiCF$_3$SO$_3$. *Jurnal Teklonogi* 2015, *75*(7), 1–5.

[39] Wang, Y.,;. Ionic Transport and Dielectric Relaxation in Polymer Electrolytes. In *Dielectric Properties of Ionic Liquids. Advances in Dielectrics*; Paluch, M., Ed.; Springer: Cham, 2016; pp 131–156.

[40] Natesan, B.; Karan, N. K.; Rivera, M. B.; Aliev, F. M.; Katiyar, R. S. Segmental Relaxation and Ion Transport in Polymer Electrolyte Films by Dielectric Spectroscopy. *J. Non-Cryst. Solids.* 2006, *352*, 5205–5209. DOI: 10.1016/j.jnoncrysol.2006.01.138.

[41] Ramya, C. S.; Selvasekarapandian, S.; Hirankumar, G.; Savitha, T.; Angelo, P. C. Investigation on Dielectric Relaxations of PVP–NH$_4$SCN Polymer Electrolyte. *J. Non-Cryst. Solids.* 2008, *354*, 1494–1502. DOI: 10.1016/j.jnoncrysol.2007.08.038.

[42] Woo, H. J.; Majid, S. R.; Arof, A. K. Dielectric Properties and Morphology of Polymer Electrolyte Based on Poly (3-caprolactone) and Ammonium Thiocyanate. *Mater. Chem. Phys.* 2012, *134*, 755–761. DOI: 10.1016/j.matchemphys.2012.03.064.

[43] Senthil Kumar, P.; Sakunthala, A.; Reddy, M. V.; Moni, P. Structural, Morphological, Electrical and Electrochemical Study on Plasticized PVdF-HFP/PEMA Blended Polymer Electrolyte for Lithium Polymer Battery Application. *Solid State Ionics.* 2018, *319*, 256–265. DOI: 10.1016/j.ssi.2018.02.022.

[44] Baskaran, R.; Selvasekarapandian, S.; Kuwata, N.; Kawamura, J.; Hattori, T. AC Impedance, DSC and FT-

IR Investigations on (X)pvac–(1 – x)PVdF Blends with LiClO$_4$. *Mater. Chem. Phys.* 2006, *98*, 55–61. DOI: 10.1016/j.matchemphys.2005.08.063.

[45] Shukur, M. F.; Ibrahim, F. M.; Majid, N. A.; Ithnin, R.; Kadir, M. F. Z. Electrical Analysis of Amorphous Corn Starch-based Polymer Electrolyte Membranes Doped with LiI. *Phys. Scr.* 2013, *88*, 025601. DOI: 10.1088/0031-8949/88/02/025601.

[46] Balaji Bhargav, P.; Madhu Mohan, V.; Sharma, A. K.; Rao, V. V. R. N. Structural and Electrical Studies of Sodium Iodide Doped Poly (Vinyl Alcohol) Polymer Electrolyte Films for Their Application in Electrochemical Cells. *Ionics.* 2007, *13*, 173–178. DOI: 10.1007/s11581-007-0102-2.

[47] Wang, Z.; Tang, Z. Characterization of the Polymer Electrolyte Based on the Blend of Poly(vinylidene Fluoride-co-hexafluoropropylene) and Poly(vinyl Pyrrolidone) for Lithium Ion Battery. *Mater. Chem. Phys.* 2003, *82*, 16–20. DOI: 10.1016/S0254-0584(03)00241-4.

[48] Veeramachineni, A. K.; Sathasivam, T.; Paramasivam, R.; Muniyandy, S.; Pushpamalar, J. Synthesis and Characterization of a Novel pH-Sensitive Aluminum Crosslinked Carboxymethyl Tragacanth Beads for Extended and Enteric Drug Delivery. *J. Polym. Environ.* 2019, *27*, 1516–1528. DOI: 10.1007/s10924-019-01448-5.

[49] Hosaini, M.; Hemmati, K.; Ghaemy, M. Synthesis of Nanohydrogels Based on Tragacanth Gum Biopolymer and Investigation of Swelling and Drug Delivery. *Int. J. Biol. Macromol.* 2016, *82*, 806–815. DOI: 10.1016/j.ijbiomac.2015.09.067.